

Preparation dependent surface structure of NiAl(100)

Sam Coates¹, Abdullah Al-Mahboob¹, Ronan McGrath¹ and Hem Raj Sharma¹

¹Department of Physics and Surface Science Research Centre, University of Liverpool, Liverpool L69 3BX, UK

E-mail: sgscoat2@liv.ac.uk, h.r.sharma@liv.ac.uk

Abstract. The dependence of surface structure formation on preparation conditions of NiAl(100) has been investigated by Scanning Tunnelling Microscopy (STM), Low Energy Electron Diffraction (LEED) and Density Functional Theory (DFT). STM and LEED have been used to study the surface after sputtering, low temperature annealing ($T < 500\text{K}$) and high temperature annealing ($500\text{K} < T < 1000\text{K}$). A (1×1) phase is observed both after sputtering and low T annealing, with STM images indicating the formation of row structures - the density of which appears dependent on annealing time. A $c(\sqrt{2} \times 3\sqrt{2})R45^\circ$ regime is detected upon higher T annealing - forming two, orthogonal, row-based domains. STM simulation produced using DFT explains the origin of one of the domains - a defect based structure with a dominant Ni density of states contribution.

1. Introduction

Nickel-Aluminium (NiAl) is a periodic CsCl-type intermetallic alloy which has been routinely investigated due to its advantageous physical properties such as high melting temperature, high strength, and good oxidation resistance. As such, NiAl alloys have been used as a base in superalloys for applications in, for example, corrosion resistant coatings and turbine blades [1]. Additionally, NiAl makes for an attractive and appropriate system for research on the general phenomena in ordered alloys due to its simplistic crystallographic structure and, by natural extension, the surface reconstructions produced from bulk termination [1]. The NiAl(100), (110) and (111) surface terminations can be regarded as prototypical systems for studying oxide growth and nanocluster formation in intermetallic compounds – an area of research with potential for applications in catalysis and electronic devices [2–6]. As such, a deep understanding of the surface structure of NiAl is imperative when considering the implications of such research.

The NiAl(100), (110) and (111) surface terminations, both clean and oxidised, have been investigated using a variety of techniques such as Low Energy Electron Diffraction (LEED) [4, 7, 9], Density Function Theory [10, 14] and Neutral Impact Collision Ion Scattering Spectroscopy (NICISS) [9]. Of specific interest here is the NiAl(100) termination - the (100) plane ideally produces alternate A–B–A–B layers of quadratically arranged pure Ni(A) or Al(B) atoms ($a_0 = 2.89\text{\AA}$ [8]). However, an energetically preferential reconstruction forms in an Al-terminated $c(\sqrt{2} \times 3\sqrt{2})R45^\circ$ regime when NiAl is annealed within a temperature range of 500 - 1000K [7, 8]. A (1×1) phase can be produced either by annealing at $T < 500\text{K}$ (Al terminated) or at $T > 1000\text{K}$ (Ni terminated) [7, 8]. Geometric optimisation of a defect rich NiAl(100) surface using Density Functional Theory (DFT) has revealed the origin of the reconstruction - concluding that there are two equally favourable defect-based atomic arrangements [10]. The

first is a structure described as Ni antisites along every third row in the (011) direction, with corresponding vacancies in the Ni layer below - known as the ‘double defect’ surface from now onwards. The second is a ‘single defect’ regime solely exhibiting the Ni vacancies within the subsurface layer. The structures are shown in figure 3d) and e) respectively. The reconstruction is, energetically, the most stable surface structure [10].

Using STM, LEED, and DFT, both phases of the NiAl(100) surface have been studied. Presented here are new data from each stage of sample preparation in an effort to uncover how atomic surface structure is affected by such preparation techniques, and to explain the origin of both surface phases. NiAl has been studied as part of a larger programme looking at adsorption and thin film structure dependence on substrate structural complexity. This will include complex and quasicrystalline Al-based intermetallics, such as Al₉Co₂ and the 10-fold Al-Ni-Co.

2. Experimental Method

A NiAl(100) single crystal was polished to a mirror finish before solvent washing. A clean surface was prepared by Ar⁺ sputtering for 20-30 minutes at pressures of $\sim 2.5 \times 10^{-5}$ mbar, followed by annealing at temperatures dependent on surface selection ($T < 500\text{K}$ for (1×1), $T = 600 - 800\text{K}$ for reconstruction) at pressures below 5×10^{-10} mbar. The sputtering conditions were chosen to remove surface and subsurface ordering. Surface cleanliness and structural determination were verified using LEED and STM at room temperature. All bias voltages used in STM measurements are with respect to the sample. STM simulations were completed using CASTEP [11], employing the Perdew-Burke-Ernzerhof generalized gradient approximation functional [12].

3. Results and Discussion

3.1. Sputtered surface

To understand the NiAl(100) surface formation and the full effect of the preparation methods, the sputtered surface was investigated. The (1×1) diffraction pattern shown in figure 1a) (confirmed by comparison to Cu(111)) indicates long range order across the surface, despite the heavy sputtering treatment. Figure 1b) shows terrace formation after sputtering, with figure 1c) showing a magnified area of a terrace. Island features are observed with an RMS roughness of 0.14 nm. Line profile analysis (labelled 1 and 2) indicates that these islands are Al-Al or Ni-Ni, based on step heights of $\sim 3\text{\AA}$ ($\simeq a$).

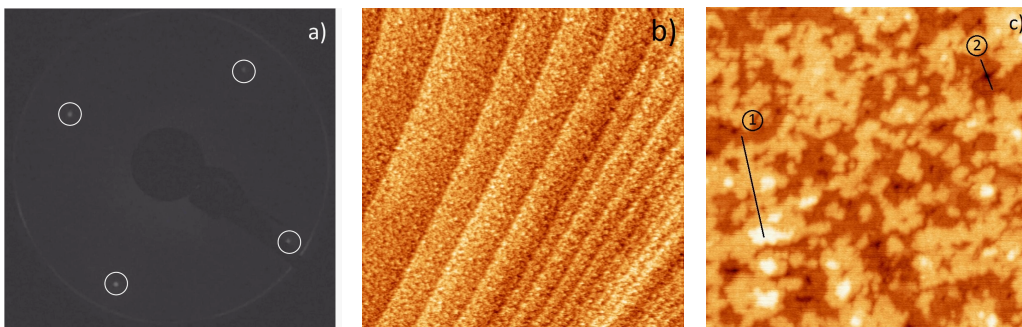


Figure 1: a) LEED pattern ($E_e = 50$ eV) from the sputtered NiAl(100) surface, producing a (1×1) diffraction pattern b) 500×500 nm² STM image ($V_b = 2000$ mV, $I_t = 270$ pA) exhibiting terraces c) 100×100 nm² STM image ($V_b = 1750$ mV) with labelled line profiles used to measure step heights of islands

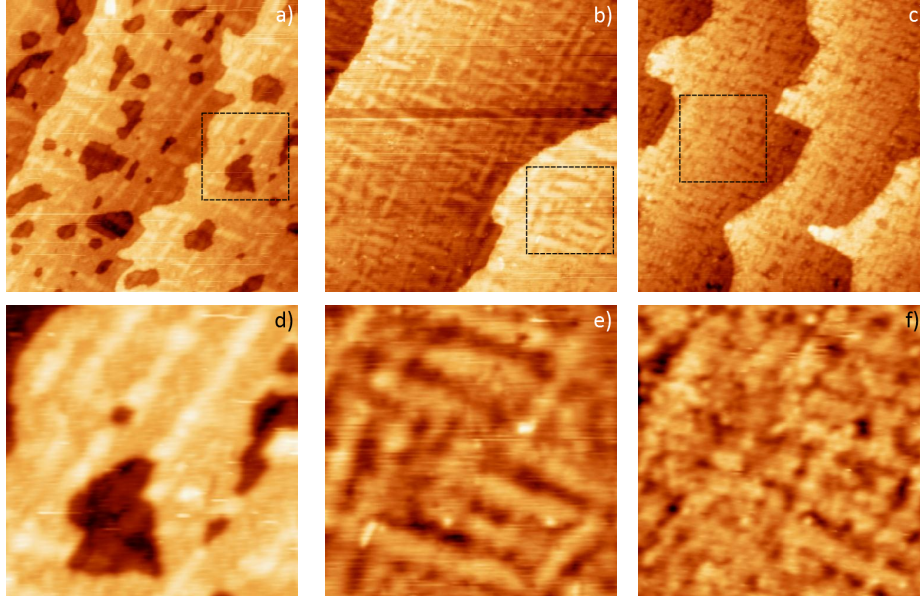


Figure 2: Series of STM images taken from different annealing preparation conditions. a) $100 \times 100 \text{ nm}^2$ STM image ($V_b = -500 \text{ mV}$, $I_t = 270 \text{ pA}$) annealing temperature $T = 420 \text{ K}$, b) $100 \times 100 \text{ nm}^2$ ($V_b = 2000 \text{ mV}$, $I_t = 270 \text{ pA}$), $T = 470 \text{ K}$, c) $100 \times 100 \text{ nm}^2$ ($V_b = 150 \text{ mV}$, $I_t = 270 \text{ pA}$), $T = 480 \text{ K}$, d-f) show $32 \times 32 \text{ nm}^2$ sections taken from highlighted regions in a-c) respectively

3.2. Low temperature annealed surface

Figure 2) shows a collection of STM scans from the (1×1) NiAl(100) surface (as verified by LEED, figure 3a)); all images are produced by annealing NiAl(100) below the reconstruction transition temperature, 500 K [9], for increasingly longer amounts of time – 2a) 20 min, b) 40 min, c) 60 min. Terraces are formed in each procedure, although 2a) exhibits a high concentration of large defects in addition to roughened step edges. The non-square shape of these defects indicates either that the annealing temperature or length of annealing time was insufficient to produce a surface in equilibrium. In all 3 scans ‘row’ structures appear in two orthogonal directions and are highlighted by enlarged images 2d-f) – the density of these structures appears to increase with increasing annealing time. In fact, upon annealing for a long time (over 12 hours) at $T < 500 \text{ K}$, the surface reconstructs into its $c(\sqrt{2} \times 3\sqrt{2})R45^\circ$ phase - indicating that the appearance of these rows is a precursor to the formation of the reconstruction.

3.3. Reconstructed surface

Upon annealing at $500 \text{ K} < T < 900 \text{ K}$ the NiAl(100) surface reconstructs into the aforementioned $c(\sqrt{2} \times 3\sqrt{2})R45^\circ$ regime. Figures 3a) and b) show the LEED patterns from the (1×1) and reconstructed surface structure phases respectively. Included in figure 3c) is a LEED simulation of the reconstruction for clarity, where two domains oriented 90° to each other are clearly visible.

STM data from this surface also appears to exhibit two orthogonal domains, as shown in 3f) and highlighted by a dashed line. To the left of the line a defined row structure is observed with separation $6.1 \pm 0.2 \text{ \AA}$, whilst inter-atomic separation along these rows is difficult to resolve. The domain to the right of the line again exhibits row structure, yet separation between these rows appears to vary between $\sim 4.5\text{-}5.5 \text{ \AA}$. Additionally, ordering between adjacent rows appears to be arbitrary, as consecutive rows are shifted along their axis, causing a ‘wavy’ effect. The possible origin of the left-hand domain has been obtained by simulating the electron density of the double defect reconstruction as seen by an STM tip, using DFT; figure 3h). Here, the double defect structure has been replicated over 3 atomic layers – an Al termination with Ni double

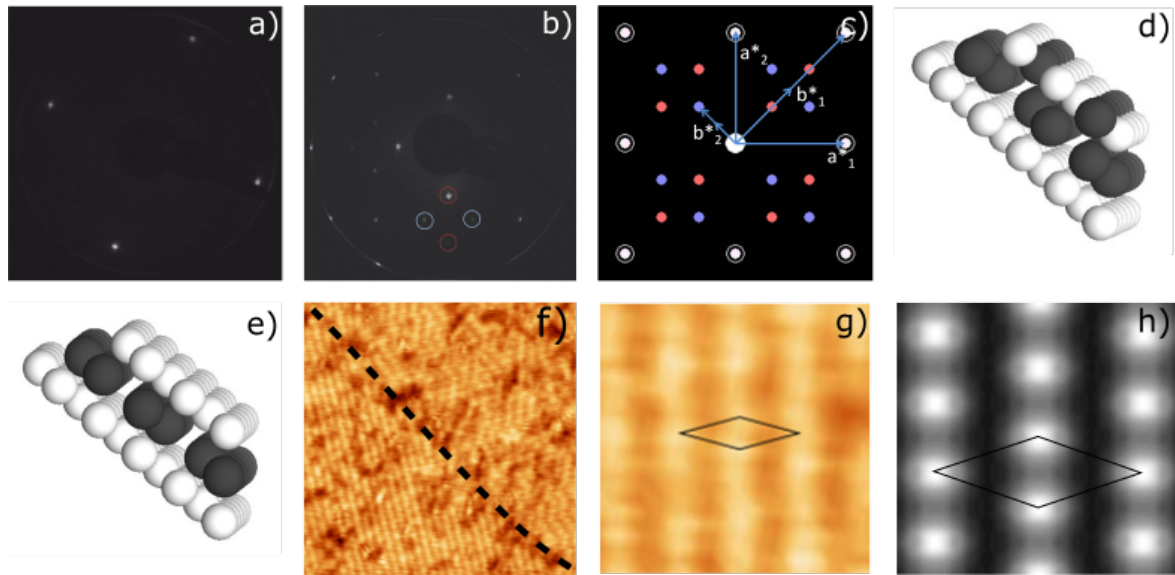


Figure 3: a) (1×1) LEED pattern ($E_e = 50$ eV) produced from NiAl(100) annealed at 470K, b) $c(\sqrt{2} \times 3\sqrt{2})R45^\circ$ LEED pattern ($E_e = 52$ eV) produced from the (100) surface, annealed at 640K, c) simulated LEED pattern of the reconstruction, where red and blue dots correspond to two orthogonal domains [13], d) double defect structure e) single defect structure f) $15 \times 15 \text{ nm}^2$ STM image with two clearly observable domains, g) $3.0 \times 2.5 \text{ nm}^2$ region with proposed unit cell highlighted h) simulated STM from double defect structure, using parameters equal to those used in the physical STM. Proposed unit cell highlighted

defects within the top 2 layers, with a pure Al layer underneath. The virtual tip is placed $\sim 3\text{\AA}$ from the surface, with an applied bias of 175mV (probing unoccupied states) - equal to that used in the physical experiment. The STM simulation produced correlates with the STM data, and can be described as the Ni density of states (DOS) dominating at the surface, producing the defined row structure as described above. DOS calculations confirm a dominant Ni d band within NiAl [15].

4. Conclusion

NiAl(100) surface formation under various preparation conditions has been studied. The (1×1) surface ordering is maintained after heavy sputtering treatment, despite a morphologically rough surface – as evidenced by LEED. Annealing the sample at $T < 500\text{K}$ produces a (1×1) surface, with orthogonal ‘row’ islands observed in STM – the density of which appears to increase with annealing time. Surface reconstruction to a $c(\sqrt{2} \times 3\sqrt{2})R45^\circ$ structure occurs after annealing at $T > \sim 800\text{K}$, which is in part attributed to a Ni based double defect structure in the subsurface, as shown by DFT calculations. Further studies will focus on the formation of islands on the (1×1) surface, including their part in formation of the reconstruction. In addition, the origin of the second domain in the reconstructed surface will be explored.

References

- [1] Miracle D B, 1993 *Acta metall. mater.* **41** 649 – 84
- [2] Qin H, Chen X, Li L, Sutter P W and Zhou G 2014 *PNAS.* E103 – 09
- [3] Cai N, Qin H, Tong X, Zhou G 2013 *Surface Science* **618** 20 – 26
- [4] Jaeger R M, et al. 1991 *Surface Science* **259** 235 – 52
- [5] Luo M F, Chiang C I, Shiu H W, Sartale S D and Kuo C C 2005 *Nanotechnology* **17** 360 – 7
- [6] Franchy R, Masuch J and Gassmann P 1996 *Applied Surface Science* **93** 317 – 27
- [7] Mullins D R, Overbury S H 1987 *Surface Science* **199** 141 – 153
- [8] Blum R P, Ahlbehrendt D, Niehus H 1996 *Surface Science* **366** 107 – 120
- [9] Niehus H, Raunau W, Besocke K, Spitzl R and Comsa G 1990 *Surface Science* **225** L8 – L14
- [10] Lerch D, Dössel K, Hammer L and Müller S 2009 *J. Phys.: Condens. Matter* **21** 134007 (6pp)
- [11] Clark S J et al. 2005 *Zeitschrift fuer Kristallographie* **220** 567 – 70

- [12] Perdew J P, Burke K and Ernzerhof M 1996 *Phys. Rev. Lett.* **77** 3856
- [13] <http://www.fhi-berlin.mpg.de/KHsoftware/LEEDpat/>
- [14] Müller S 2003 *J. Phys.: Condens. Matter* **15** 1429 – 1500
- [15] Lui S C, Davenport J W, Plummer E W, Zehner D M, and Fernando G W 1990 *Phys. Rev. B* **42** 1582 – 1597